Electronic Supplementary Material (ESI) for Organic & Biomolecular Chemistry.

Exploring the reversal of enantioselectivity on a Zinc-dependent Alcohol Dehydrogenase

Miguel A. Maria-Solano,[a] Adrian Romero-Rivera[a], Sílvia Osuna*[a]

SUPPORTING INFORMATION

COMPUTATIONAL METHODS WITH FULL REFERENCES

Molecular Dynamics Simulations. MD simulations in explicit water were performed using AMBER 16 package[1] and starting from the PDB structure: 1YKF.[2] The I86A and W110T variants were generated using the mutagenesis tool included in PyMOL (http://www.pymol.org). Parameters for substrate **1a** for the MD simulations were generated within the *antechamber* module of AMBER 16 using the general AMBER force field (GAFF),[3] with partial charges set to fit the electrostatic potential generated at the B3LYP/6-31G(d) level by the restrained electrostatic potential (RESP) model.[4] The charges were calculated according to the Merz-Singh-Kollman scheme[5, 6] using Gaussian 09.[7] Amino acid protonation states were predicted using the H++ server (http://biophysics.cs.vt.edu/H++).[8] We have used the bonded model for Zn and the residues of the first coordination sphere, in particular we used the Seminario approach[9] to obtain the metal parameters needed for the simulation as implemented in Prof. Ryde program.[10] The optimization, frequencies and charge calculations to obtain the parameters was done at the B3LYP/6-31G(d) level using Gaussian 09.[7] The parameters for NAD(P)H were extracted from previous studies by Prof. Ryde.[11, 12] The Wild-Type (WT) enzyme (PDB: 1YKF) and variants were solvated in a pre-equilibrated truncated cuboid box with a 10-Å buffer of TIP3P[13] water molecules using the AMBER16 *leap* module, resulting in the addition of *ca.* 9,000 solvent molecules. The system was neutralized by addition of explicit counterions (Na^+ and Cl^-). All calculations were done using a modification of the *ff*99SB force field (*ff1*4SB).[14] A two-stage geometry optimization approach was performed. The first stage minimizes the positions of solvent molecules and ions imposing positional restraints on solute by a harmonic potential with a force constant of 500 kcal mol^{-1} $Å^{-2}$, and the second stage is an unrestrained minimization of all the atoms in the simulation cell. The systems are gently heated using six 50-ps steps, incrementing the temperature 50 K each step (0–300 K) under constant volume and periodic boundary conditions. Water molecules were treated with the SHAKE algorithm such that the angle between the hydrogen atoms is kept fixed. Long-range electrostatic effects were modeled using the particle-mesh-Ewald method.[15] An 8-Å cutoff was applied to Lennard-Jones and electrostatic interactions. Harmonic restraints of 10 kcal/mol were applied to the solute, and the Langevin equilibration scheme was used to control and equalize the temperature. The time step was kept at 1 fs during the heating stages, allowing potential inhomogeneities to self-adjust. Each system was then equilibrated without restrains for 2 ns with a 2-fs timestep at a constant pressure of 1 atm and temperature of 300 K. After the systems were equilibrated in the NPT ensemble, 3 independent five hundred nanosecond MD simulations were performed under the NVT ensemble and periodic-boundary conditions.

The *theozyme* calculations for the hydride transfer step were performed at the B3LYP/6-31G(d) level of theory using Gaussian 09.[7] Active site volume calculations were performed with the computational tool POVME 2.0.[16]

Table S1. Volume calculated (Å^3) on the different variants on the small and big pocket without **1a** in the 3 most populated clusters using POVME[16].

	WT TbSADH						TbSADH^{I86A}						TbSADH^{W110T}					
Pockets	Prelog			Anti-Prelog			Prelog			Anti-Prelog			Prelog			Anti-Prelog		
	C_0	C_1	C_2	C_0	C_1	C_2	C_0	C_1	C_2	C_0	C_1	C_2	C_0	C_1	C_2	C_0	C_1	C_2
Small	78	62	68	77	79	72	91	86	84	93	98	83	-	-	-	-	-	-
Large	97	99	83	104	104	115	-	-	-	-	-	-	197	145	154	174	168	155

Table S2. Calculation of the %ee of *pro*-(R) and *pro*-(S) conformations. *Calculation of the conformations taking into account distances lower than 4.5 Å (closer the catalytic distance) and their corresponding angles are used to classify the *pro*-(R) and *pro*-(S) conformations. $C_{R/S}$ is the productive number of *pro*-(R) and *pro*-(S) conformations, N is the total number of frames in the MD simulation.

$$\%ee = \left(\frac{P_R - P_S}{P_R + P_S}\right) x100 \qquad P_R = \frac{C_R}{N} \qquad P_S = \frac{C_S}{N} \qquad \text{eq. 1}$$

Variants		R*	S*	% ee (R)	% ee (S)
WT TbSADH	*Pro*-(S)	0.36	0.20	29	-
	Pro-(R)	0.68	0.08	79	-
TbSADH^{I86A}	*Pro*-(S)	0.02	0.51	-	92
	Pro-(R)	0.69	0.16	62	-
TbSADH^{W110T}	*Pro*-(S)	0.33	0.12	47	-
	Pro-(R)	0.45	0.03	88	-

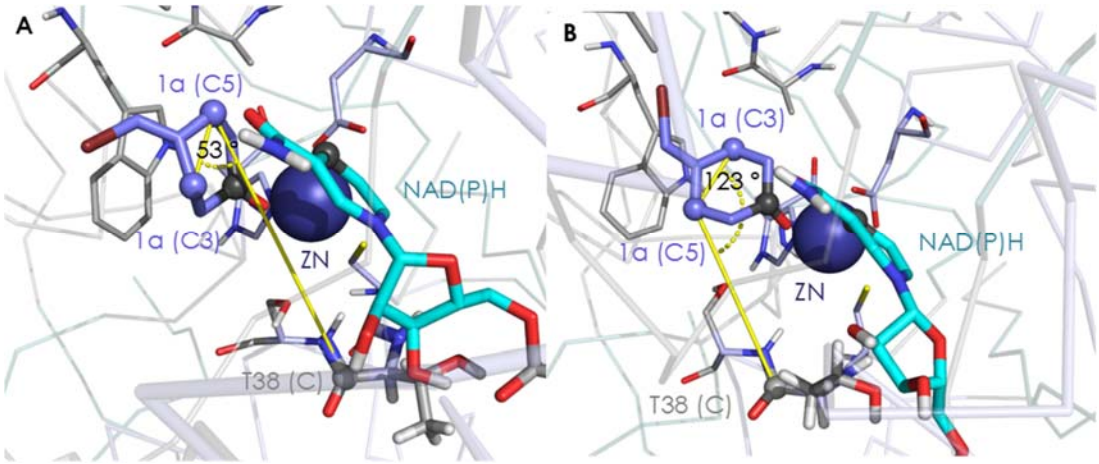

Figure S1. Representation of the selected angle between T38 (C), 1a (C5) and 1a (C3) for the determination of *pro*-(S) (A) and *pro*-(R) (B) orientations. The atoms involved in the angle and in the hydride transfer are shown in spheres.

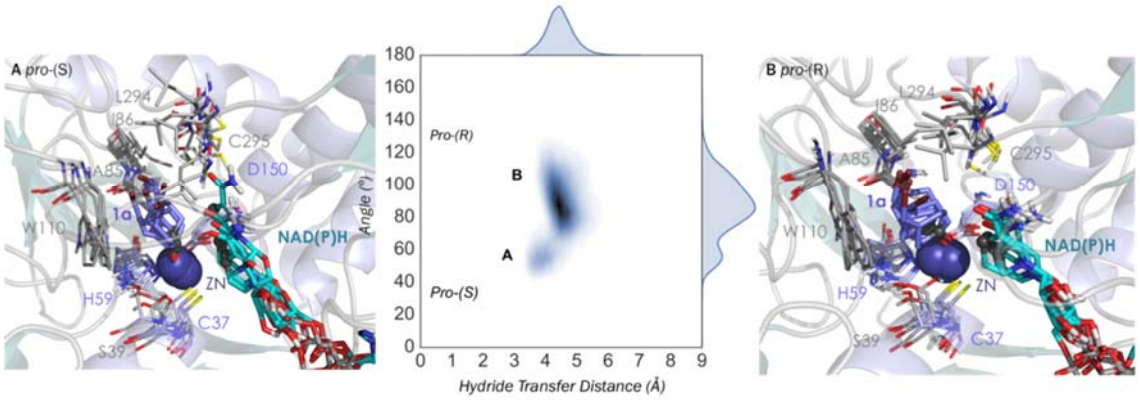

Figure S2. Representation of some representative snapshots of the different conformational states sampled along the MD simulations for TbSADH starting from the *pro*-(S) orientation of **1a**. The histogram of the hydride transfer distance together with the *pro*-(R)/*pro*-(S) angle (detailed in Figure S1) is displayed.

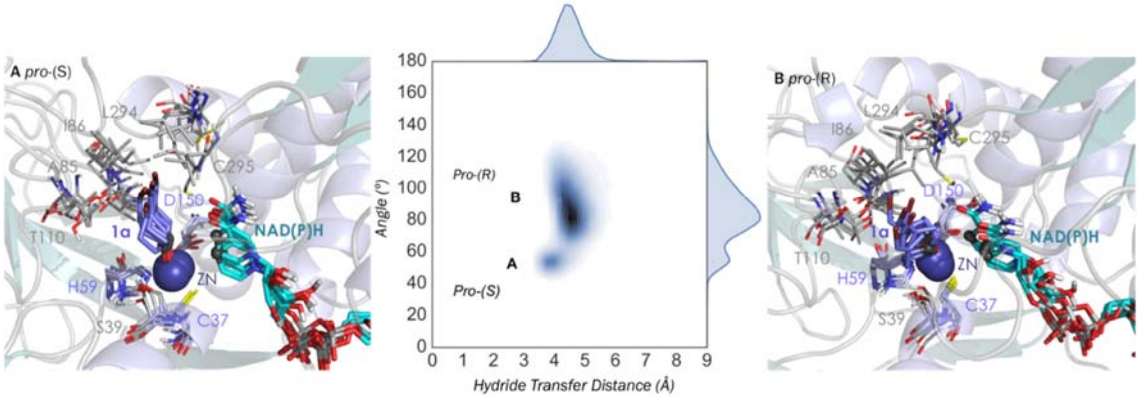

Figure S3. Representation of some representative snapshots of the different conformational states sampled along the MD simulations for the TbSADH^{W110T} starting from the *pro*-(S) (in blue) orientations of **1a**. The histogram of the hydride transfer distance together with the *pro*-(R)/*pro*-(S) angle (detailed in Figure S1) is displayed.

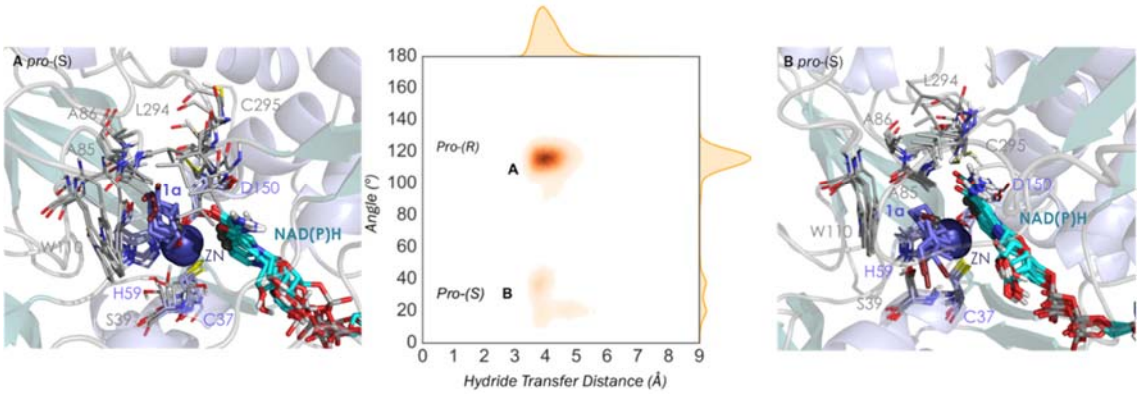

Figure S4. Representation of some representative snapshots of the different conformational states sampled along the MD simulations for TbSADH^{I86A} starting from the *pro*-(R) (in orange) orientations of **1a**. The histogram of the hydride transfer distance together with the *pro*-(R)/*pro*-(S) angle (detailed in Figure S1) is displayed.

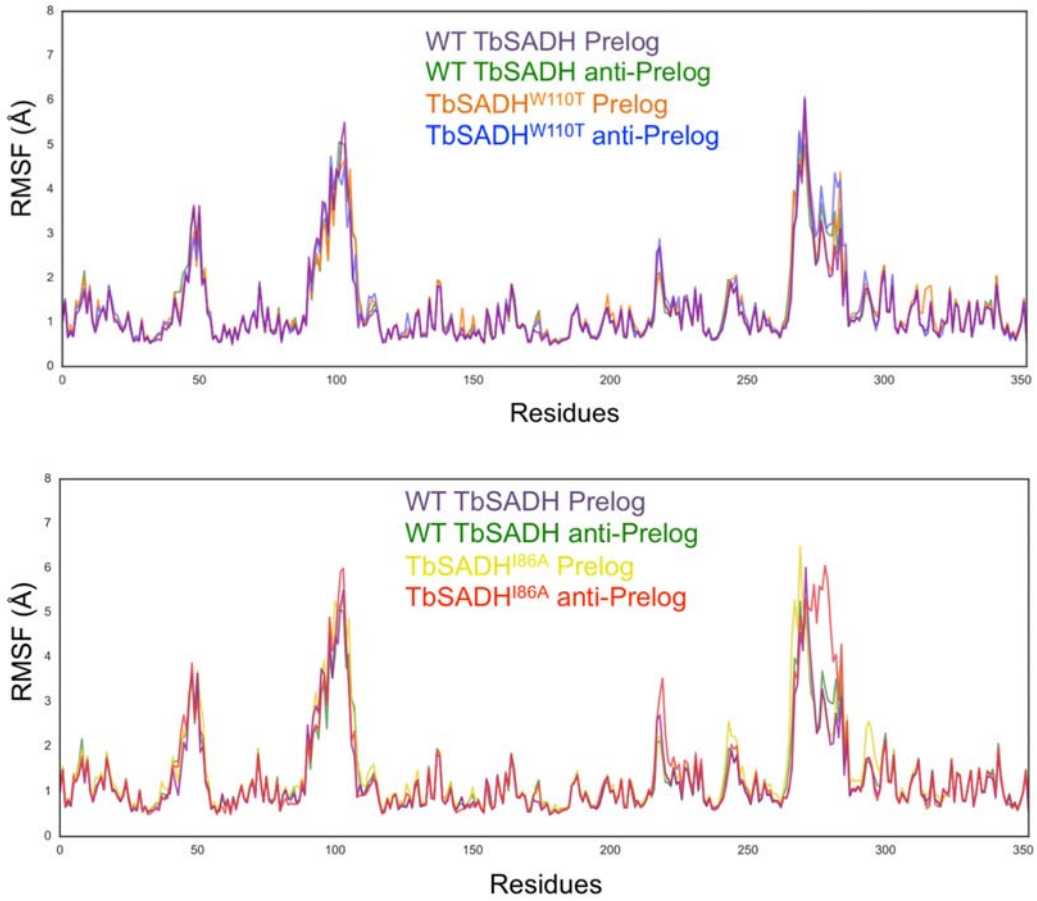

Figure S5. Root Mean Square Fluctuation (RMSF, in Å) along the microsecond timescale MD simulations.

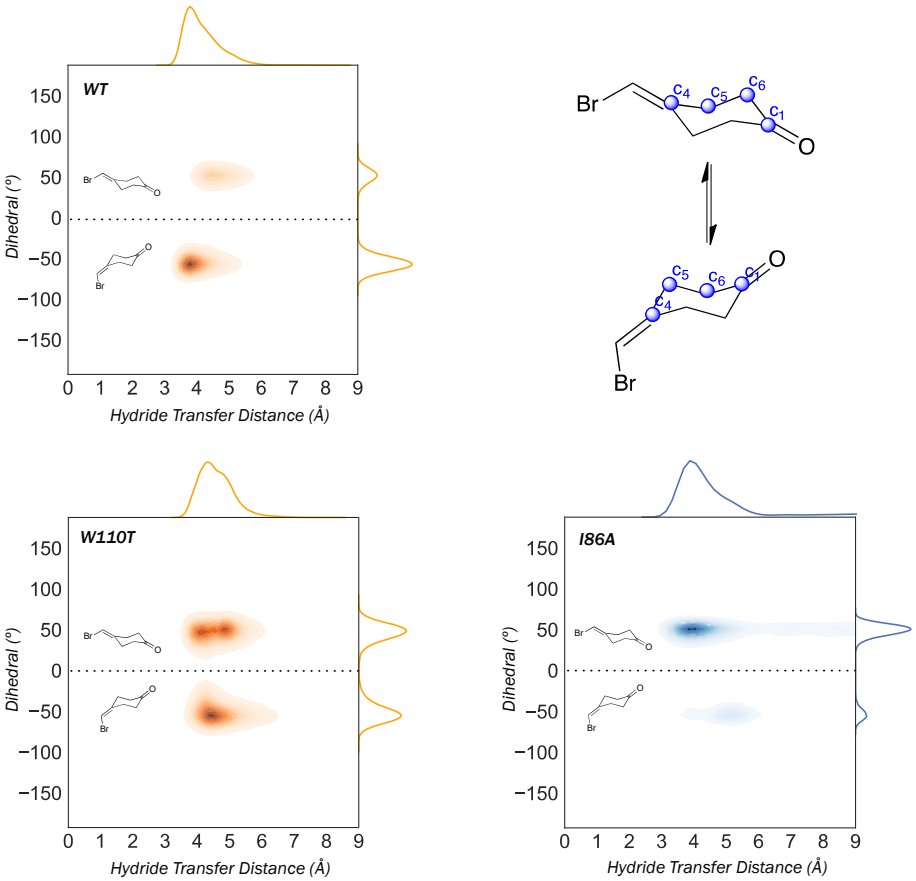

Figure S6. Representation of **1a** conformations sampled along the MD simulations for the TbSADH^{W110T}, TbSADH and TbSADH^{I86A}. The histogram of the hydride transfer distance together with the dihedral of the chair of **1a** (C1, C6, C5, C4) is displayed.

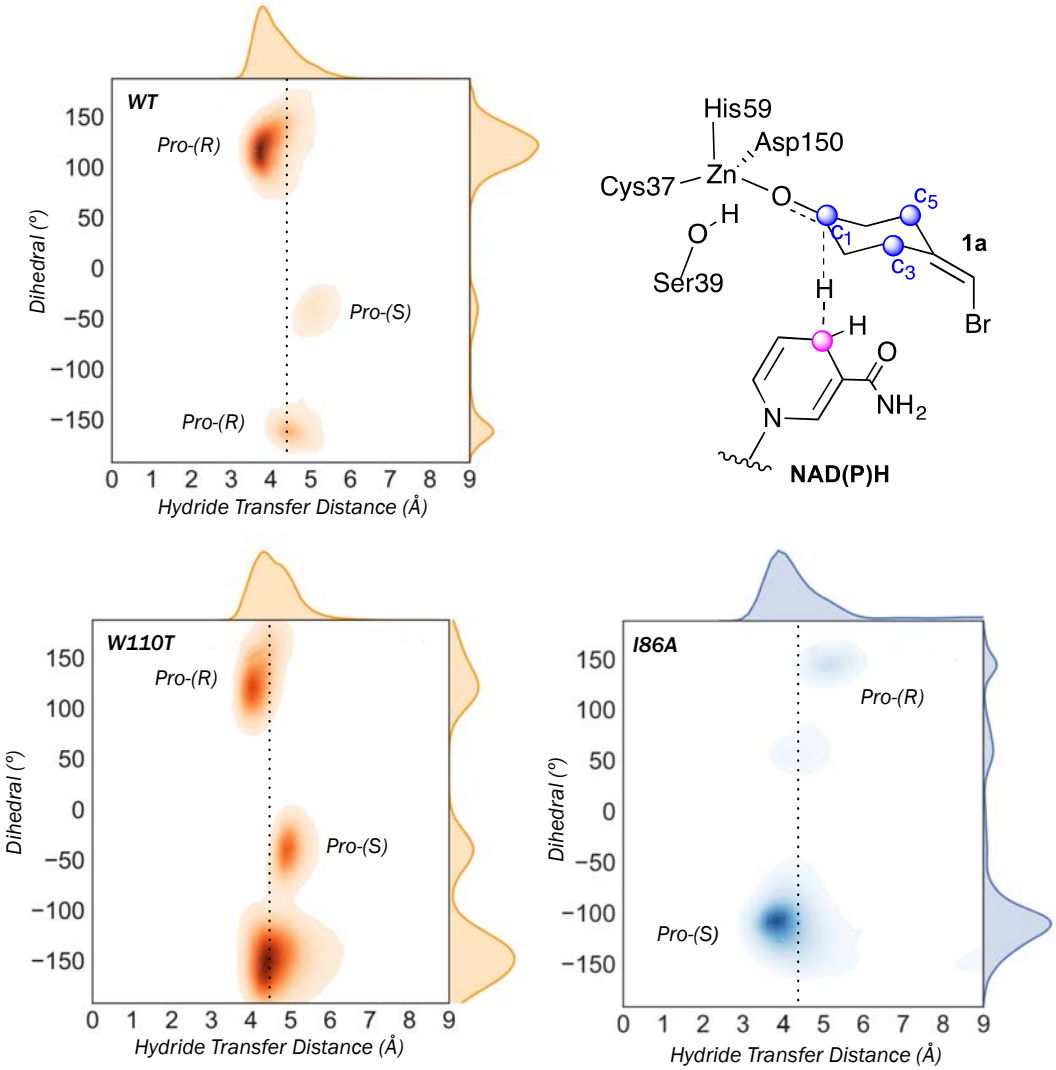

Figure S7. Representation of the *pro*-(R)/*pro*-(S) conformations sampled along the MD simulations for WT TbSADH, TbSADH^{W110T}, and TbSADH^{I86A}. The histogram of the hydride transfer distance together with the dihedral of **1a** (C3, C5, C1) and C (NAD(P)H, *i.e.* hydride transfer carbon) is displayed. Atoms used to calculate the dihedral angle are shown in spheres.

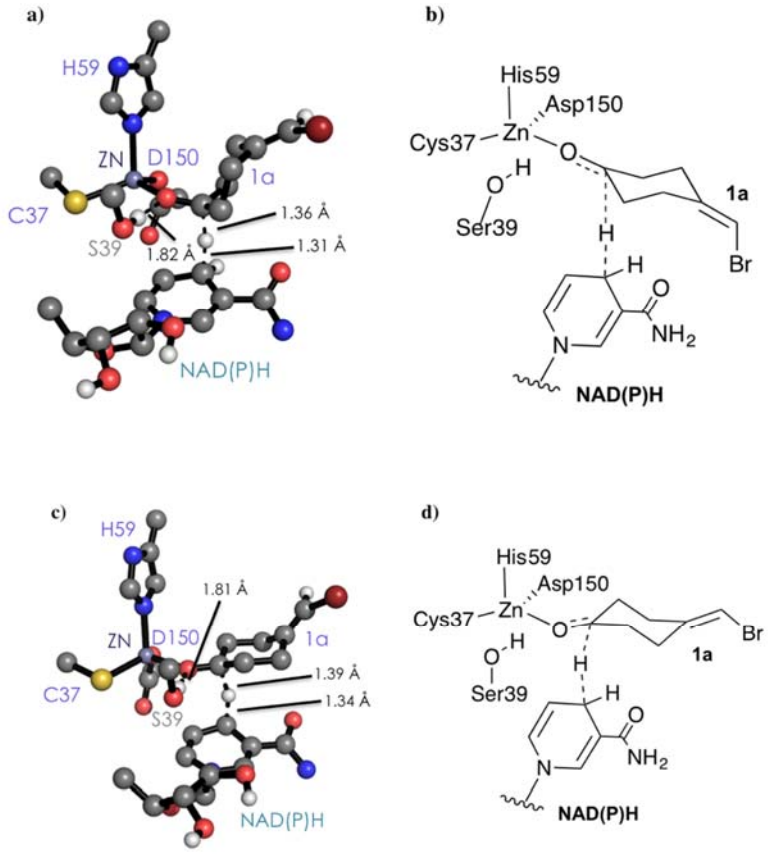

Figure S8. TS calculations for equatorial (a) and axial (c) attacks, followed by their respective chemdraw representations.

Dataset S1. Optimized Cartesian coordinates for the TS corresponding to the equatorial attack.

C	1.787437	1.125009	1.433691
C	0.015505	1.967248	-0.183447
C	1.122809	2.568934	-1.088241
C	2.894615	1.747238	0.542756
H	-0.838897	1.657653	-0.792277
H	1.476635	1.853329	2.190716
H	2.170144	0.234133	1.938962
H	1.387609	1.825490	-1.853071
H	0.742288	3.452516	-1.606558
H	3.275205	0.970779	-0.135035
H	3.733844	2.068696	1.168569
H	-0.318991	2.726421	0.531164
C	2.352647	2.898518	-0.280793
C	0.578201	0.763950	0.572228
C	2.952933	4.087893	-0.219666
O	0.581346	-0.371383	-0.087695
Br	2.388460	5.642809	-1.200481
H	3.827454	4.296858	0.383700
C	1.337269	-5.247790	-0.621626
S	0.210596	-3.785782	-0.722782
C	-0.872518	-0.465519	-3.256821
O	-1.473963	-0.641159	-1.980598

C	6.946485	-1.435586	-1.363926
C	5.477721	-1.701110	-1.352834
C	4.546963	-1.690375	-0.345452
N	4.759984	-2.037201	-2.489192
C	3.464276	-2.213680	-2.150074
N	3.298887	-2.010788	-0.851535
C	2.755433	-2.574335	4.270317
C	1.821436	-2.543972	3.063093
O	0.624535	-2.838857	3.192478
O	2.399601	-2.181645	1.958585
N	-3.750303	-0.095630	0.998582
C	-3.489546	1.110464	1.579755
C	-2.357536	1.332747	2.316805
C	-1.324152	0.299188	2.379866
C	-1.764437	-1.019127	1.946210
C	-2.909803	-1.162566	1.230498
C	-2.075935	2.637565	2.974554
N	-3.141798	3.443769	3.253770
O	-0.913187	2.979713	3.216944
C	-4.924850	-0.200903	0.097054
C	-4.641117	0.374531	-1.314182
C	-5.601567	-0.463551	-2.170026
C	-5.553070	-1.835896	-1.482626
C	-4.496909	-2.784499	-2.036125
O	-4.849593	1.764386	-1.407051
O	-6.874407	0.171331	-2.029336
O	-5.278064	-1.545139	-0.073702
H	-3.508582	-2.313094	-2.066781
H	-4.436724	-3.681205	-1.411138
H	-5.732816	0.363004	0.581066
H	-3.601113	0.166014	-1.583104
H	-5.299072	-0.512115	-3.221237
H	-6.541811	-2.304256	-1.509488
H	-5.810234	1.869444	-1.548005
H	-7.456974	-0.130036	-2.743517
H	-0.376227	0.630674	1.533465
H	-0.679058	0.333259	3.259464
H	-4.236209	1.877120	1.407530
H	-4.066920	3.055710	3.375455
H	-2.943270	4.286888	3.777629
H	-1.150990	-1.883066	2.177741
H	-3.259836	-2.109878	0.845674
H	-1.664506	-0.537294	-4.008084
H	-0.391866	0.518453	-3.359174
H	-0.123479	-1.241105	-3.471628
H	-4.768892	-3.096070	-3.050938
H	7.198306	-0.588643	-2.013107
H	7.287507	-1.200280	-0.352668
H	7.510860	-2.305773	-1.719306
H	5.138852	-2.136542	-3.422390
H	-0.764386	-0.580118	-1.299600
H	2.308655	-5.029591	-1.074908
H	1.498531	-5.555106	0.416099
H	0.883700	-6.083743	-1.161826
H	4.683076	-1.487739	0.705664
H	2.689781	-2.489611	-2.849811
H	3.144690	-1.567976	4.463005

H	2.232927	-2.934338	5.159132
H	3.617603	-3.218485	4.066375
Zn	1.534876	-2.112381	0.196976

Dataset S2. Optimized Cartesian coordinates for the TS corresponding to the axial attack

N	4.653884	-2.347811	-2.466331
N	3.213009	-2.195351	-0.817006
C	1.164852	-5.461163	-0.321457
C	-0.895516	-0.885553	-3.303573
C	6.822327	-1.515092	-1.457850
C	5.368599	-1.846952	-1.390258
C	4.450716	-1.760820	-0.374846
C	3.372545	-2.542822	-2.085272
C	2.635038	-2.661780	4.318216
C	1.711581	-2.629025	3.103192
O	-1.522512	-0.912624	-2.028384
O	0.506219	-2.892778	3.227441
O	2.305988	-2.301919	1.997152
S	0.119748	-3.969492	-0.640993
Zn	1.447057	-2.282020	0.236115
H	-1.677177	-1.008361	-4.059227
H	-0.381688	0.068198	-3.494031
H	-0.169108	-1.701707	-3.423772
H	7.025552	-0.746396	-2.212786
H	7.160452	-1.136878	-0.489893
H	7.426262	-2.395091	-1.708774
H	5.025580	-2.542566	-3.387368
H	-0.823913	-0.797690	-1.342589
H	2.171799	-5.331520	-0.729308
H	1.246968	-5.668546	0.749693
H	0.704799	-6.327347	-0.805607
H	4.594064	-1.428554	0.641848
H	2.602668	-2.935619	-2.732325
H	3.066512	-1.667896	4.483028
H	2.092199	-2.972660	5.213314
H	3.469658	-3.348595	4.139973
N	-3.553408	0.137370	0.962291
N	-2.988358	3.827792	2.918280
C	-3.291436	1.392947	1.421827
C	-2.136381	1.693675	2.095243
C	-1.078713	0.689182	2.194281
C	-1.521746	-0.670154	1.919383
C	-2.694875	-0.893682	1.269072
C	-1.899649	3.030968	2.703476
C	-4.769569	-0.070285	0.137630
C	-4.551635	0.305425	-1.349258
C	-5.578360	-0.609532	-2.032185
C	-5.526970	-1.879920	-1.169943
C	-4.546185	-2.939353	-1.656119
O	-0.754143	3.410146	2.973010
O	-4.734843	1.676344	-1.615120
O	-6.825868	0.079193	-1.912396
O	-5.140817	-1.419966	0.166374
H	-3.546495	-2.519409	-1.810929
H	-4.475929	-3.747565	-0.921047
H	-5.547672	0.566018	0.578945

H	-3.533369	0.032050	-1.642442
H	-5.336981	-0.807986	-3.081435
H	-6.531319	-2.303309	-1.069745
H	-5.699347	1.789478	-1.718690
H	-7.451777	-0.288966	-2.554956
H	-0.157006	0.921432	1.254308
H	-0.393335	0.820223	3.032631
H	-4.061618	2.128246	1.220565
H	-3.908570	3.427880	3.039049
H	-2.815819	4.689607	3.420673
H	-0.908606	-1.511739	2.226072
H	-3.051803	-1.877960	1.001003
H	-4.898042	-3.369468	-2.600653
C	0.314843	1.763893	-0.766831
C	0.749232	0.687008	0.231558
C	2.069186	0.963273	0.951861
C	2.221863	2.420667	1.426356
C	1.908935	3.390576	0.305343
C	0.535154	3.212038	-0.287643
C	2.821251	4.286471	-0.071039
O	0.508604	-0.544446	-0.145952
Br	2.558589	5.580799	-1.471522
H	2.186986	0.264718	1.786633
H	0.912719	1.586914	-1.673253
H	-0.731659	1.600059	-1.045813
H	1.515102	2.611597	2.244311
H	3.232496	2.576803	1.817614
H	-0.196429	3.454396	0.492475
H	0.370451	3.902922	-1.118263
H	2.867069	0.728376	0.231653
H	3.800580	4.385869	0.380189

References:

1. D. A. Case, T. A. Darden, T. E. Cheatham, C. L. Simmerling, J. Wang, R. E. Duke, R. Luo, M. Crowley, R. C. Walker, W. Zhang, K. M. Merz, B. Wang, S. Hayik, A. Roitberg, G. Seabra, I. Kolossváry, K. F. Wong, F. Paesani, J. Vanicek, X. Wu, S. R. Brozell, T. Steinbrecher, H. Gohlke, L. Yang, C. Tan, J. Mongan, V. Hornak, G. Cui, D. H. Mathews, M. G. Seetin, C. Sagui, V. Babin and P. A. Kollman, *AMBER 16, University of California, San Francisco, 2016*.
2. Y. Korkhin, A. J. Kalb, M. Peretz, O. Bogin, Y. Burstein and F. Frolow, *J. Mol. Biol.*, 1998, **278**, 967-981.
3. J. Wang, R. M. Wolf, J. W. Caldwell, P. A. Kollman and D. A. Case, *J. Comput. Chem.*, 2004, **25**, 1157-1174.
4. C. I. Bayly, P. Cieplak, W. Cornell and P. A. Kollman, *J. Phys. Chem.*, 1993, **97**, 10269-10280.
5. U. C. Singh and P. A. Kollman, *J. Comput. Chem.*, 1984, **5**, 129-145.
6. B. H. Besler, K. M. Merz and P. A. Kollman, *J. Comput. Chem.*, 1990, **11**, 431-439.
7. G. W. T. M. J. Frisch, H. B. Schlegel, G. E. Scuseria, M. A. Robb, J. R. Cheeseman, G. Scalmani, V. Barone, G. A. Petersson, H. Nakatsuji, X. Li, M. Caricato, A. Marenich, J. Bloino, B. G. Janesko, R. Gomperts, B. Mennucci, H. P. Hratchian, J. V. Ortiz, A. F. Izmaylov, J. L. Sonnenberg, D. Williams-Young, F. Ding, F. Lipparini, F. Egidi, J. Goings, B. Peng, A. Petrone, T. Henderson, D. Ranasinghe, V. G. Zakrzewski, J. Gao, N. Rega, G. Zheng, W. Liang, M. Hada, M. Ehara, K. Toyota, R. Fukuda, J. Hasegawa,

M. Ishida, T. Nakajima, Y. Honda, O. Kitao, H. Nakai, T. Vreven, K. Throssell, J. A. Montgomery, Jr., J. E. Peralta, F. Ogliaro, M. Bearpark, J. J. Heyd, E. Brothers, K. N. Kudin, V. N. Staroverov, T. Keith, R. Kobayashi, J. Normand, K. Raghavachari, A. Rendell, J. C. Burant, S. S. Iyengar, J. Tomasi, M. Cossi, J. M. Millam, M. Klene, C. Adamo, R. Cammi, J. W. Ochterski, R. L. Martin, K. Morokuma, O. Farkas, J. B. Foresman, and D. J. Fox, *Inc.: Wallingford, CT*, 2009.

8. R. Anandakrishnan, B. Aguilar and A. V. Onufriev, *Nucleic Acids Res.*, 2012, **40**, W537-W541.
9. J. M. Seminario, *Int. J. Quantum Chem.*, 1996, **60**, 1271-1277.
10. L. Hu and U. Ryde, *J. Chem. Theory Comput.*, 2011, **7**, 2452-2463.
11. U. Ryde, *Proteins*, 1995, **21**, 40-56.
12. U. Ryde, *Protein Sci.*, 1995, **4**, 1124-1132.
13. W. L. Jorgensen, J. Chandrasekhar, J. D. Madura, R. W. Impey and M. L. Klein, *J. Chem. Phys.*, 1983, **79**, 926-935.
14. V. Hornak, R. Abel, A. Okur, B. Strockbine, A. Roitberg and C. Simmerling, *Proteins*, 2006, **65**, 712-725.
15. T. Darden, D. York and L. Pedersen, *J. Chem. Phys.*, 1993, **98**, 10089-10092.
16. J. D. Durrant, L. Votapka, J. Sørensen and R. E. Amaro, *J. Chem. Theory Comput.*, 2014, **10**, 5047-5056.